Available online at www.sciencedirect.com
SCIENCE DIRECT®
Journal of Molecular Catalysis A: Chemical 228 (2005) 195–202
JOURNAL OF MOLECULAR CATALYSIS A: CHEMICAL
www.elsevier.com/locate/molcata

Theoretical study of nickel porphyrinate derivatives related to catalyst dopant in the oil industry

Isidoro García-Cruz[a,*], José Manuel Martínez-Magadán[a], Fernando Alvarez-Ramirez[a], Roberto Salcedo[a,b], Francesc Illas[a,c,*]

[a] *Programa de Ingeniería Molecular, Instituto Mexicano del Petróleo, Eje Central Lázaro Cárdenas 152, Colonia San Bartolo Atepehuacan, México D.F. 07730, Mexico*
[b] *Instituto de Investigaciones en Materiales, Ciudad Universitaria, Universidad Nacional Autónoma de México, México D.F. 04510, Mexico*
[c] *Departament de Química Física i Centre especial de Recerca en Química Teòrica, Universitat de Barcelona i Parc Científic de Barcelona, C/Martí i Franquès 1, 08028 Barcelona, Spain*

Available online 5 November 2004

Abstract

Density functional calculations have been carried out for several Ni porphyrinates representative of the most common form in which this metal is present in crude oil. A detailed study of the molecular and electronic structure is presented including the description of the low lying electronic states leading to the well known Q and Soret bands in the optical spectra. The reliability of the present study is confirmed by comparison to experimental data. It is found that presence of different substituents does not largely affect the electronic structure of the nickel porphyrin moiety including the energy excitation required to promote these molecules to the low lying electronic states. It is proposed that these promoted Ni-porphyrin derivatives can participate in poisoning catalysts like zeolites and metallic sulfides. However, the need for electronic promotion in Ni-porphyrinate derivatives indicates that this family of compounds is likely to be less active as catalyst poison than other metals like V, in agreement with experimental evidence.

Keywords: Electronic structure; Nickel-porphyrin; DFT calculations; Crude oil

1. Introduction

The presence of metals in crude oils has been long known and it is also associated to several technological problems [1]. Different metals can be present in crude oil depending on the geological and geographical origin of the sample: up to 27 elements were found in the analysis of ash of US oil crudes [2]. Nickel and vanadium are no doubt the most abundant metals in crude oil and can reach concentrations ranging from 250 up to 2000 ppm for Ni and V, respectively. Typically V is found in higher concentration than Ni [3]. It is customary to classify the chemical forms in which these metals are found in crude oil in terms of porphyrinic and non-porphyrinic [3,4]. The porphyrin fraction is the largest; it is well defined and identified by several characteristic spectroscopic features [5–7]. The non-porphyrinic term is used to describe all forms in which metals can be found in oil crude other than porphyrinic. The porphyrinic fraction may involve easily 40–50% of the total amount of V and Ni contained in average crude oils [8] and the remaining of these two metals is found in a much less characterized way [9]. Hence, one must not be surprised that the terms petroporphyrins (or geoporphyrins) is commonly used in the oil industry to describe the most common chemical form of trace metals in crude oil [10]. The presence of metals in crude oil has negative and positive effects because they can either poison the catalyst or, on the contrary, catalyze some reaction of interest [11]. It has been reported that both Ni and V interfere with the refining processes, their presence being related to severe deactivation of many heterogeneous catalysts, mainly zeolites and metal sulphides used in several

* Corresponding authors.
E-mail addresses: igarcia@imp.mx (I. García-Cruz), francesc.illas@ub.edu (F. Illas).

1381-1169/$ – see front matter © 2004 Elsevier B.V. All rights reserved.
doi:10.1016/j.molcata.2004.09.038

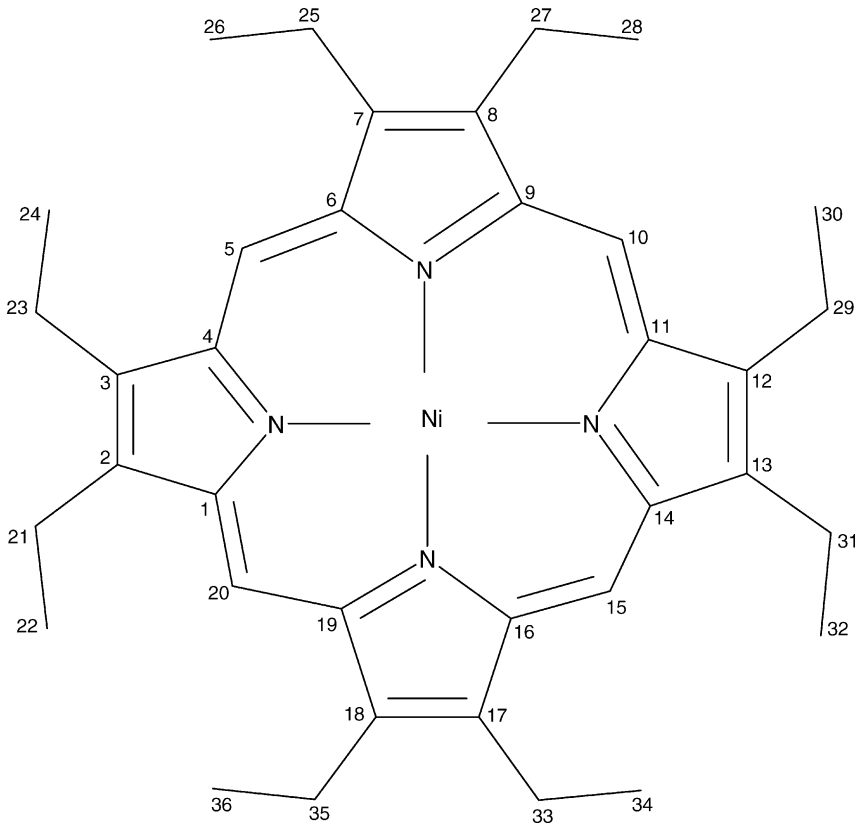

Fig. 1. Schematic representation of the Ni-octaethylporphyrinate (compound **2**) and the different substituted compounds used in this work.

steps of the fluid catalytic cracking, with a concomitant strong economic detriment in the oil industry [12]. Moreover, it has been found that V is much more destructive than Ni although the reasons for such behavior remain largely unknown. At least in part, catalyst deactivation is due to metal deposition and also in this case the deposition rate is larger for V than for Ni [9].

Several spectroscopic and theoretical studies exist which deal with Ni-porphyrins having either lateral aliphatic or aromatic branches [4–16]. However, these studies attempt to relate changes in structure with some features regarding their biological and photophysical activity [17]. Therefore, a detailed description of the molecular and electronic structure of some Ni-petroporphyrin complexes appears as highly desirable. The main goal of the present work is precisely the study of various Ni-porphyrin derivatives either present in crude oil or used as models in laboratory experiments. In particular, reliable molecular structures are reported and their electronic structure analyzed with special emphasis on the effect of substituents. To this end, accurate density functional theory (DFT) based calculations have been carried out for a series of four Ni-porphyrin compounds starting with the simple Ni-porphyrinate (compound **1**) for which various detailed theoretical studies carried out at different levels of theory exist [18,19] including the analysis of the low lying excited states [19]. Two Ni-porphyrinate derivatives have been included which are representative of the main different families of petroporphyrins; etioporphyrins and *meso* or β-cycloalkaneporphyrins; these are Ni-octaethylporphyrinate (compound **2**) and Ni-deoxophylloerythroetio porphyrinate (compound **3**), respectively. Finally, Ni-tetraphenylporphyrinate (compound **4**) is also included since it is also widely employed as a model compound in demetallation studies [20]. On the other hand, compounds **2** and **4** are often used as models in the experimental research of petroporphyrins [9,20,21] whereas compound **3** is one of the real form in which Ni-porphyrins are found in crude oil [9]. A schematic representation of compound **2** is given in Fig. 1. The atoms in this figure are numbered following the biogenetic numeration. The positions 1, 4, 6, 9, 11, 14, 16, 19 are α-positions, positions 2, 3, 7, 8, 12, 13, 17 and 18 are β-positions and the positions 5, 10, 15 and 20 are the *meso*-positions. The most stable conformer reported by Stoll et al. [16] from B3LYP calculation—within a 6-31G* basis set for C, H and N and the Ahlrich's valence triple-ζ (VTZ) for nickel basis sets—has been selected. It is expected that the microscopic information reported in this work can be useful in finding out reasonable hypothesis about catalyst poison activity of Ni-porphyrins and thus to contribute to the design of effective demetallation processes for heavy oil processes.

2. Computational details

For computational convenience, the optimum geometry of the four compounds described above has been carried out using density functional theory (DFT) within the gradient corrected Becke–Perdew (BP) [22] whereas all the energy based analysis have been carried out using the B3LYP exchange-correlation functional [23]. The BP calculations all-electrons are explicitly considered and the electron density is expanded in double-ζ numerical basis set augmented by polarization functions, this is referred to as DNP. These basis sets are given as numerical values on a sufficiently large grid centered on each atom. For each system, a complete geometry optimization has been carried out for the ground state closed-shell electronic structure configuration as well as for the lowest triplet state and the corresponding cation. For the ground state, the calculations are spin restricted whereas for the cation and for the triplet states the spin unrestricted implementation of the Kohn–Sham DFT formalism is used. This set of calculations has been carried out using the DMol3 computer program [24].

Using the Becke–Perdew exchange-correlation and the DNP optimized geometry—hereafter referred to as BP/DNP—single-point calculations have been carried out using the B3LYP exchange-correlation functional [23] which has proven to provide more accurate energy values. In principle, B3LYP performs better for organic compounds although it has also been shown to perform very well in transition metal elements containing compounds although no transition metal compounds were included in the data set used in the fit [25–28]. The B3LYP calculations have been carried out using standard Contracted Gaussian Type Orbitals (CGTO) basis sets; 6-31G** for all atoms except for Ni for which the small core effective core potential (ECP) of Hay and Wadt has been selected together with the standard double-ζ basis Gaussian basis set [29], normally referred to as LANL2DZ. For Ni-porphyrinate (compound **1**), the B3LYP calculations involve a total of 418 CGTO functions whereas the calculations corresponding to Ni-octaethylporphyrinate (compound **2**), Ni-deoxophylloerythroetio porphyrinate (compound **3**) and Ni-tetraphenylporphyrinate (compound **4**) are more demanding and involve 802, 692 and 834 CGTOs, respectively. The B3LYP calculations have been carried out using the Gaussian98 suite of programs [30].

From the B3LYP calculations several properties are obtained and analyzed such as core-level shifts for the N atoms on the pyrrolic ring, singlet–triplet energy differences and the excitation energy for the lowest allowed singlet–singlet transition which can be directly compared to the electronic spectra of porphyrins and in particular to the so-called Q and B (or Soret) bands [5,7,19]. The latter has been obtained using time dependent DFT (TD-DFT) as implemented in Gaussian98 and using again the B3LYP model for the exchange-correlation functional. TD-DFT is based in the Kohn–Sham formulation of DFT and makes use of the eigenvalues and eigenvectors of the Kohn–Sham equations thus permitting a rather simple interpretation of the excited levels in terms of one-electron excitations [19]. The excitation energies are calculated from the poles of the frequency-dependent polarizability and the oscillator strengths from the residues. In order to compare with experiment we assume that excitations follow the Franck–Condon principle. Hence, TD-DFT excitation energies are computed using only the ground state geometry.

3. Results and discussion

In order to assess the accuracy of the present computational approach for the optimized structural parameters, the present calculated values for Ni-porphyrinate and Ni-octaethylporphyrinate, as obtained from the BP/DNP computational scheme, are compared to those predicted from X-ray diffraction measurements [31–34] (Table 1). From the results reported in Table 1 it appears that the BP/DNP method is able to quantitatively describe the bond lengths and bond angles of both compounds **1** and **2**. The BP/DNP values for compounds **3** and **4** are reported in Table 2, values for the compounds **1** and **2** are also reported in Table 2 for comparison. The final optimized geometries of the four compounds are schematically depicted in Fig. 2. For compound **1** the present results are in very good agreement with the BP results reported by Baerends et al. using a triple-ζ basis set of Slater type orbitals [19]. Both sets of calculated results are also in agreement with

Table 1
Experimental and computed geometrical parameters (Å and °) of the Ni-porphyrinate (compound **1**) and Ni-octaethylporphyrinate molecule (compound **2**)

Parameter	Compound **1**		Compound **2**	
	X-ray[a]	BP/DNP	X-ray[b]	BP/DNP
Bond length (Å)				
Ni—N	1.951	1.974	1.961	1.960
C_1—N	1.379	1.383	1.376	1.380
C_1—C_2	1.435	1.439	1.450	1.450
C_2—C_3	1.371	1.364	1.369	1.377
C_4—C_5			1.383	1.387
C_2—C_{21}			1.504	1.502
C_{21}—C_{22}	1.347	1.383	1.542	1.542
Angles bond (°)				
N—Ni—N	90.0	90.0	90.0	90.1
Ni—N—C_1	127.8	127.7	127.6	127.3
N—C_1—C_2	111.0	111.0	111.4	111.1
N—C_4—C_5	125.4	125.4	124.8	124.7
C_1—N—C_4	104.3	104.6	104.8	105.2
C_1—C_2—C_3	106.8	106.7	106.2	106.3
C_1—C_2—C_{21}			125.3	125.0
C_2—C_3—C_{23}	123.6	124.4	128.5	128.5
C_2—C_{21}—C_{22}		128.9	113.7	114.0
C_3—C_4—C_5	123.5	123.6	123.7	124.0
C_4—C_5—C_6	123.6	123.8	124.0	124.0
C_1—N—N—C_{11}	1.7	0.0	19.8	27.8

The calculated values correspond to the BP/DNP level of theory.
[a] Ref. [31].
[b] Refs. [32–34].

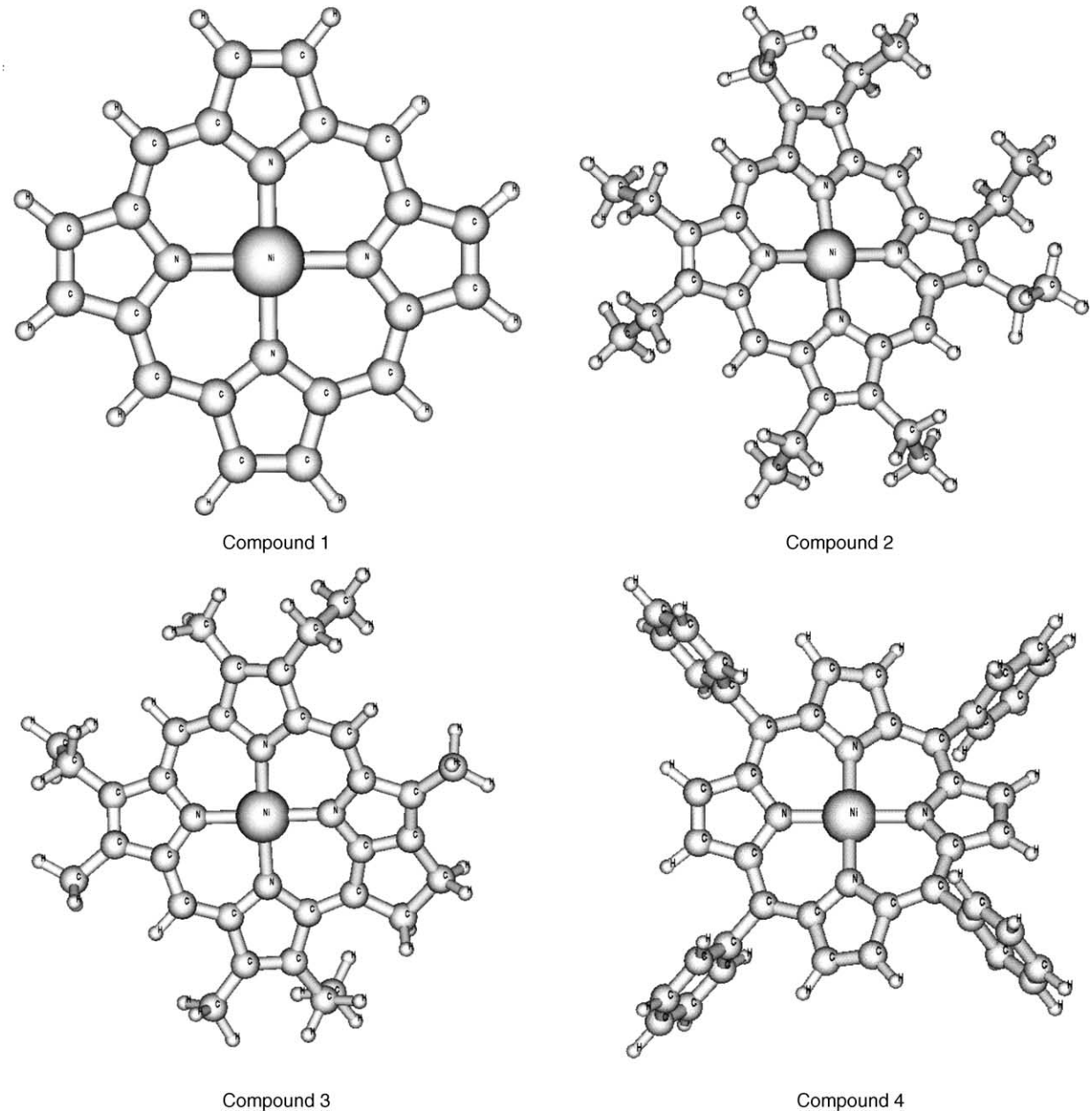

Fig. 2. Optimized geometries of the Ni-porphyrinate compounds studied in the present work as obtained at the BP/DNP level theory.

experimental results with a maximum deviation in the Ni–N distance of 0.02 Å between calculated and experimental values (see [19] and references therein).

Ni-porphyrinate is totally planar hence exhibiting a marked difference with respect to the analogous vanadyl compound which has been shown to have a dome shape [35]. However, the other Ni-porphyrinates studied in the present work also exhibit a slight non-planar shape. In any case, the tendency to strain out of the planarity of this kind of molecules is well known and confirmed by several X-ray analyses [31–34]. The origin of this strain has been attributed to the reduced space of the porphyrin molecule cavity and also to the presence of peripheral substituents [36]. The nature of this deviation has also triggered several theoretical studies [37]. Therefore, it is not surprising at all that the substituted molecules exhibit a ruffle deviation and that the numerical value of the angle corresponding to the strain in this deviation depends on the nature of the substituent (see C_1–N–N–C_{11} in Table 2). It appears that the largest deviation from planarity occurs in the case of phenyl substituents whereas in both aliphatic cases a similar strain is predicted. This feature could be attributed to a large increase in the electronic density near the metal center caused by the presence of the aromatic rings.

To analyze the electronic structure we first comment on the Mulliken population analysis as predicted from both BP

Table 2
Optimized BP/DNP geometrical parameters (Å and °) of Ni-porphyrinates (compounds **1**–**4**) in the closed-shell electronic ground state

	Compound			
	1	**2**	**3**	**4**
Bond length (Å)				
Ni—N	1.974	1.960	1.955	1.934
C_1—N	1.383	1.380	1.380	1.383
C_1—C_2	1.439	1.450	1.453	1.441
C_2—C_3	1.364	1.377	1.375	1.365
C_2—C_{21}		1.502	1.498	
C_2—H_{21}	1.085			1.084
C_4—C_5	1.383	1.387	1.389	1.397
Angles bond (°)				
N—Ni—N	90.0	90.1	90.9	90.0
Ni—N—C_1	127.7	127.3	127.5	127.2
N—C_1—C_2	111.0	111.1	110.9	110.3
N—C_4—C_5	125.4	124.7	124.8	125.2
C_1—N—C_4	104.6	105.2	105.4	105.6
C_1—C_2—C_3	106.7	106.3	106.5	106.9
C_1—C_2—C_{21}		125.0	124.9	
C_1—C_2—H_{21}	124.4			124.6
C_2—C_3—C_{23}		128.5	128.6	
C_2—C_3—H_{23}	128.9			128.4
C_3—C_4—C_5	123.6	124.0	124.1	124.1
C_4—C_5—C_6	123.8	124.0	124.2	121.5
C_1—N—N—C_{11}	0.0	27.8	25.4	36.0

and B3LYP calculations (Table 3). In all cases a rather large positive charge (∼0.5 eV) is predicted in Ni, the BP and B3LYP predictions being very close to each other. This positive charge on Ni is accompanied by a negative charge in the N atoms of the pyrrolic rings which again is very similar for the four different compounds and for the different functionals. Therefore, while this simple analysis is able to show the marked electrophilic character of the metallocycle moiety, it does not permit to discriminate the effect of the different substitutents. In order to have a more detailed picture we have analyzed the N(1s) core levels and compared to those of the pyrrole. Accurate core-level binding energies can be obtained from the total Kohn–Sham energy differences of the neutral molecule and the molecule with a core hole [38]. However, qualitative trends can also be obtained from the orbital energies of a Hartree–Fock calculation [39]. According to the Koopman's theorem the negative value of these one-electron energies are approximate ionization potentials which are indeed very useful to establish trends initial state effects [39]. In principle, the lack of an equivalent of the Koopman's theorem in DFT does not allow one to use the Kohn–Sham orbital energies as an estimate of the core-level binding energies. Nevertheless, recent theoretical analysis and numerical results by Chong et al. strongly suggest to interpret the energies of the occupied KS orbitals as approximate but rather accurate *relaxed* ionization potentials [40]. These would include not only initial state effects but also the final stated effects caused by the electronic relaxation in response to the presence of the core hole. In fact, the N(1s) binding energy estimated for pyrrole from the Kohn–Sham orbital energy is 382.02 and 391.50 eV at the BP and B3LYP levels, reasonably close to the experimental value of 406.2 eV [41], specially for the B3LYP method. Notice that the Hartree–Fock value for the pyrrole N(1s) estimated from the Koopman's theorem is 424.8 eV, quite far from the DFT values, and becomes 406.3 eV when computed from a ΔSCF calculation; the relaxation energy amounts to 18.5 eV [42,43]. Clearly, the DFT values are closer to the experimental value as expected from the analysis of Chong et al. [40]. In any case, the meaningful analysis of the present results concerns the comparison of the core-level binding energies for the different substituted porphyrins and of the core-level shift with respect to pyrrole. The former also indicates that the electronic structure of the porphyrin moiety is almost unaffected by the substituents, the latter is consistent with this appreciation and also with the Mulliken analysis. The N(1s) level becomes less bound and shift towards higher energies although for the different compounds the shift is also similar.

Table 3
Mulliken charges on Ni and N, Q(Ni) and Q(N), core-level N(1s) ionization energy and core-level N(1s) with respect to pyrrole (Δ) for the four Ni-porphyrinate compounds studied in the present work as predicted by the BP and B3LYP methods

Method	Compound			
	1	**2**	**3**	**4**
Q(Ni)				
BP	0.60	0.58	0.57	0.57
B3LYP	0.60	0.54	0.52	0.56
Q(N)				
BP	−0.47	−0.48	−0.48	−0.46
B3LYP	−0.62	−0.61	−0.61	−0.58
N(1s) (Ev)				
BP	381.42	381.00	380.97	381.27
B3LYP	390.30	389.97	389.95	389.99
Δ (eV)				
BP	0.60	1.02	1.05	0.75
B3LYP	1.20	1.53	1.55	1.51

The core-level energy is estimated from the corresponding Kohn–Sham eigenvalues. The N(1s) ionization energy for pyrrole is 382.02 and 391.50 eV at the BP and B3LYP levels, respectively. The experimental value is 406.2 eV.

Table 4 reports the ionization potentials of the four Ni-porphyrins studied in the present work as estimated from

Table 4
Negative of the Kohn–Sham HOMO ($-\varepsilon$), vertical (IP) and adiabatic ionization potentials (IPa) of Ni-porphyrinates (compounds **1**–**4**)

	BP			B3LYP, $-\varepsilon$
	$-\varepsilon$	IP	IPa	
Compound **1**	4.85	5.07	5.03	5.25
Compound **2**	4.49	4.26	4.19	4.82
Compound **3**	4.45	4.25	4.11	4.78
Compound **4**	4.69	4.25	4.15	4.98

IP and IPa are obtained from ΔSCF calculations, this is $-\{(E_{\text{cation}} - E_{\text{neutral}})\}$. IP uses the geometry of the neutral molecule for both species whereas IPa considers the optimum geometry of each species. All results are given in eV.

Janak's theorem [44] using the BP and B3LYP exchange-correlation functionals. This theorem ensures that, for the exact exchange-correlation functional and for infinite systems, the Kohn–Sham energy of the HOMO (ε) is the negative of the ionization potential. Since the two functionals used are approximate, the IP values have also been obtained from proper ΔSCF calculations carried out using the BP geometry of the neutral species for the neutral and cation (vertical IP) and the BP geometry of both species (adiabatic IP). For the BP functional, the IP values estimated from ε are in a qualitative agreement with the adiabatic IP values (Table 4). This fact permits to use the ε values to compare IPs of the four compounds estimated from the two functionals. The absolute values are different but they are also strongly correlated, the BP functional values being roughly 0.3 eV smaller than those arising from the B3LYP method. The absolute values of the IP of the different compounds are all in the 4–5 eV interval but with differences which are significant, the largest one corresponding to compound **1** and the smallest ones to **2** and **3** as expected from the inductive effect of the corresponding substitutents. This effect can also be observed in the net charges reported in Table 3 although the variations are again too small to be considered as significant. However, a clear trend exists between IP values and the N(1s) core-level shifts with respect to pyrrole with a correlation of ~0.9 for the B3LYP values and of 0.99 for the BP ones. The explicit relaxation of the cation orbitals at the BP/DNP level or of the cation optimized geometry introduces noticeable changes in the calculated ionization potentials and the difference between the different compounds almost disappears. Geometry optimization for the cation leads to a geometrical structure which is almost the same obtained for the neutral molecule and, consequently, the resulting adiabatic ionization potential values are only slightly smaller than the corresponding vertical values. This permits one to conclude that the initial state effects either on the core levels or on the HOMO can be used to distinguish the different substitutents. Moreover, the rather large values of these ionization potentials suggest that oxidation processes are difficult in agreement with previous findings indicating that oxidation of Ni-porphyrinate derivatives requires the use of perchlorate, a strong oxidizing agent [45]. From these results it is clear that it is unlikely that the poisoning activity of Ni-porphyrinates could be due to the presence of these species in the form of radical cations, the energy cost is too large.

Finally we consider the lowest excited states of the Ni-porphyrins studied in the present work. This is because the closed-shell nature of these compounds would suggest that to be chemically active some kind of promotion would be needed. On the other hand, the analysis of the electronic spectra of these porphyrins shows two well defined bands with weak and strong intensities indicating the existence of excited states sufficiently low in energy so as to participate in the chemistry in the conditions at which fluid catalytic cracking takes place. These are the well known Q and B (Soret) bands appearing at 2.28 and 2.22, and 3.11 and 3.22 eV for compounds **1** and **2**, respectively, although values for compound **1** were determined from the CS_2 solution spectrum (see [19] and references therein). For compound **1** a detailed analysis has been reported by Baerends et al. using TD-DFT within the statistical averaging of orbital dependent model potentials. These authors show that TD-DFT is able to quantitatively explain the low energy spectrum of compound **1** with calculated values for the Q and B bands of 2.40 and 3.23 eV and oscillator strengths of 0.0052 and 1.0214, respectively. These results strongly suggest to employ TD-DFT to study the low lying states of the rest of compounds considered in the present work. This will allow one to investigate the effect of substituents on this absorption bands. The present B3LYP for compound **1** are 2.49 and 3.48 eV for the Q and B bands with oscillator strengths of 0.004 and 0.731, respectively, very close those reported by Baerends et al. [19] (2.40 and 3.23 eV) and, hence, also in a similar agreement with experiment (2.28 and 3.11 eV). The predicted values for the Q and B bands and the corresponding oscillator strengths of the rest of compounds are reported in Table 5. For compound **2** the calculated value of 2.41 is also in very good agreement with the experimental value of 2.22 eV described above. Moreover, the excitation energy is very close to that of compound **1**, also in agreement with experimental evidence. From the data in Table 5 one can safely conclude that the effect of substituents on the optical spectrum of these four Ni-porphyrin derivatives is very small. This is important because compounds **2** and **4** are synthetic models for the Ni-geoporphyrins whereas compound **3** is one of the real components of crude oil. Finally, the excitation energy to the lowest triplet (ΔE_{ST}) as obtained from B3LYP single-point energy difference at the ground state optimized geometry was determined. Again the excitation energy corresponding to compounds **1** and **2** are very similar and lower than the one corresponding to the singlet state as usual. However, for **3** the trend in the excited singlet and triple states is reversed, the low lying singlet state being slightly lower in energy. Finally, we note that for compound **4** the lowest triplet appears at quite higher energy than for the rest of compounds. This result has to be attributed to the presence of the phenyl groups which probably provide further stability to the singlet closed-shell ground state.

Table 5
TD-DFT/B3LYP calculated values for the energy (ΔE_{SS}) and oscillator strength (f) for the excitation leading to the Q and B bands and B3LYP excitation energy (ΔE_{ST}) for the lowest triplet state as obtained from a single-point calculation of Ni-porphyrinates (compounds **1**–**4**)

	Band Q		Band B (Soret)		Triplet, ΔE_{ST}
	ΔE_{SS}	f	ΔE_{SS}	f	
Compound **1**	2.49	0.004	3.48	0.731	1.70
Compound **2**	2.41	0.022	3.34	0.794	1.70
Compound **3**	2.39	0.021	3.31	0.669	2.37
Compound **4**	2.37	0.001	3.26	1.006	3.87

All results are given in eV.

4. Conclusions

In this work the molecular and electronic structure of several Ni-compounds representative of those commonly present in petroporphyrins have been studied using DFT within the BP and B3LYP approaches. It has been found that the influence of the substituents in the molecular structure of the core of the Ni-porphyrin is very small. On the other hand, the analysis of the ground state electronic structure reveals that different substitutents have a noticeable influence on the core-level energies. It is suggested that the N(1s) core-level shift with respect to a given reference such as pyrrole can be used to monitor the presence of different compounds. Finally, TD-DFT has been used to study the lowest excitations which are present in the optical spectra of these technologically relevant compounds. For the naked Ni-porphyrin, the excitation energy and relative intensities for the Q and Soret bands are in good agreement with experiment with previous theoretical studies. For the rest of compounds there is no experimental information except for compound **2** where the predicted TD-DFT values are in nice agreement with experiment. More importantly, the excitation energies leading to the Q band and B band in compounds **1** and **2** are very similar as found in experiment, this is also found to be the case for compounds **3** and **4**. In all cases it is found that the Q and B bands appear at very close energies and hence exhibiting very low sensitivity to the presence of substitutents.

In the case of V, model studies based on density functional theory suggested that the poisoning activity of V(IV) porphyrinate arises mainly from the radical character of the V-porphyrinate arising from the vanadyl radical moiety [35]. However, it is not at all clear that a similar mechanism can hold for the Ni derivatives because of their ground state closed-shell electronic structure. In fact, the present analysis of the electronic structure suggests that the interaction of a Ni-porphyrinate with a catalyst will be very weak unless the former is promoted to a low lying excited state. The present study shows that the low lying electronic states for bare Ni-porphyrin and for the different substituted compounds considered here appear at roughly the same energies and, hence the promotion argument for different forms of Ni-petroporphyrins is supported. However, although Ni-porphyrinates can be promoted to a chemically active excited state, their reactivity towards the catalyst will be much less aggressive than that of the V-porphyrinate derivatives because the radical character of the vanadyl moiety is already active in the electronic ground state. This is indeed in agreement with the experimental evidence indicating that V is a stronger catalyst poison than Ni [13,46].

Finally, it is worth pointing out that the present study relies in the molecular and electronic structure of the isolated Ni-porphyrins. However, to build up a more realistic model of crude oil porphyrins in asphaltenic fractions both porphyrin packing and solvent effects would have to be considered.

Acknowledgments

F.I. is grateful to the DURSI of the Generalitat de Catalunya and to the Spanish Ministerio de Ciencia y Tecnologia (projects 2001SGR-00043, Distinció per a la Promoció de la Recerca Universitària and BQU2002-04029-C02-01) for financial support.

References

[1] P.H. Schipper, F.G. Dwyer, P.T. Sparrel, S. Mizrahi, J.A. Herbst, ACS Symposium Series, 194th Meeting, 1987, Chapter 5, p. 64.
[2] T.F. Yen (Ed.), The Role of Trace Metals in Petroleum, Ann Arbor Sci., Ann Arbor, MI, 1975, pp. 1–30.
[3] C.D. Person, J.B. Green, Fuel 68 (1989) 465.
[4] A. Triebs, Ann. Chem. 509 (1934) 103.
[5] M. Gouterman, in: D. Dolphin (Ed.), The Porphyrins, vol. 3, Academic Press, New York, 1979, Chapter 1.
[6] J.G. Rankin, R. Cantu, R.S. Czernuszewicz, T.D. Lash, Org. Geochem. 30 (1999) 201.
[7] J.M. Boggess, R.S. Czernuszewicz, T.D. Lash, Org. Geochem. 33 (2002) 1111.
[8] J.M. Sugihara, R.M. Bean, J. Chem. Eng. Data 7 (1962) 269.
[9] E. Furimsky, F.E. Massoth, Catal. Today 52 (1999) 381.
[10] D.H. Freeman, J.M. Quirke, T.F. Yen, A.J. Barwise, G.J. Van Berkel, Energy Fuels 4 (1990) 627, and other articles in the same special issue.
[11] B. Delmon, Catal. Lett. 22 (1993) 1.
[12] S.V. Lysenko, N.S. Norol'kov, E.A. Karakhanov, Pet. Chem. USSR 28 (1988) 110.
[13] W.P. Hettinger Jr., Catal. Today 53 (1999) 367.
[14] H.S. Eom, S.C. Jeoung, D. Kim, J.H. Ha, Y.R. Kim, J. Phys. Chem. A 101 (1997) 3661.
[15] T. Wondimagegn, A. Ghosh, J. Phys. Chem. B 104 (2000) 10858.
[16] L.K. Stoll, M.Z. Zgierski, P.M. Kozlowski, J. Phys. Chem. A 106 (2002) 170.
[17] J. Rodríguez, C. Kirmaier, D. Holten, J. Chem. Phys. 94 (1991) 6020.
[18] M.C. Piqueras, C. Mc Rohlfing, Theor. Chem. Acc. 97 (1997) 81.
[19] E.J. Baerends, G. Ricciardi, A. Rosa, S.J.A. van Gisbergen, Coord. Chem. Rev. 230 (2002) 5.
[20] Y. Shiraishi, T. Hirai, I. Komasawa, Ind. Eng. Chem. Res. 39 (2000) 1345.
[21] R.P. Rodgers, C.L. Hendrickson, M.R. Emmett, A.G. Marshall, M. Greaney, K. Qian, Can. J. Chem. 79 (2001) 546.
[22] A.D. Becke, J. Chem. Phys. 88 (1988) 2547.
[23] A.D. Becke, J. Chem. Phys. 98 (1993) 5648;
C. Lee, W. Yang, R.G. Parr, Phys. Rev. B 37 (1988) 785.
[24] B. Delley, J. Chem. Phys. 92 (1990) 508;
Cerius2 User Guide, Molecular Simulation, San Diego, 1996.
[25] A. Ricca, C.W. Bauschlicher, J. Phys. Chem. 98 (1994) 12899.
[26] T.V. Russo, R.L. Martin, P.J. Hay, J. Chem. Phys. 102 (1995) 8023.
[27] L. Rodriguez-Santiago, M. Sodupe, V. Branchadell, J. Chem. Phys. 105 (1996) 9966.
[28] P.E.M. Siegbahn, R.H. Crabtree, J. Am. Chem. Soc. 119 (1997) 3103.
[29] P.J. Hay, W.R. Wadt, J. Chem. Phys. 82 (1985) 270.
[30] M.J. Frisch, et al., Gaussian 98 Revision A.9, Gaussian, Inc., Pittsburgh, PA, 1998.
[31] W. Jentzen, I. Turowska-Tyrk, W.R. Scheidt, J.A. Shelnutt, Inorg. Chem. 35 (1996) 3559.
[32] E.F. Meyer, Acta Cryst. B 28 (1972) 2162.
[33] D.L. Cullen, E.F. Meyer, J. Am. Chem. Soc. 96 (1974) 2095.

[34] T.D. Brennan, W.R. Scheidt, J.A. Shelnut, J. Am. Chem. Soc. 110 (1988) 3919.
[35] R. Salcedo, L.M.R. Martínez, J.M. Martínez-Magadán, J. Mol. Struct. Theochem. 542 (2001) 115.
[36] W. Jentzen, I. Turowska-Tyrk, W.R. Scheidt, J.A. Shelnutt, Inorg. Chem. 35 (1996) 3539.
[37] R.J. Cheng, P.Y. Chen, T. Lowell, T. Liu, L. Noodleman, D.A. Case, J. Am. Chem. Soc. 125 (2003) 6774, and references therein.
[38] Y. Takahata, D.P. Chong, J. Electron Spectrosc. Relat. Phenom. 133 (2003) 69.
[39] P.S. Bagus, F. Illas, G. Pacchioni, F. Parmigiani, J. Electron Spectrosc. Relat. Phenom. 100 (1999) 215.
[40] D.P. Chong, O.V. Gritsenko, E.J. Baerends, J. Chem. Phys. 116 (2002) 1760.
[41] K. Siegbahn, C. Nordling, G. Johansson, J. Hedman, P.F. Heden, K. Hamrin, U. Gelius, T. Bergmark, L.O. Werme, R. Manne, Y. Baer, ESCA—Applied to Free Molecules, North-Holland, Amsterdam, 1969.
[42] P.S. Bagus, F. Illas, J. Casanovas, J.M. Jimenez-Mateos, J. Electron Spectrosc. Relat. Phenom. 83 (1997) 151.
[43] P.S. Bagus, F. Illas, J. Casanovas, Phys. Lett. 272 (1997) 168.
[44] F.K. Janak, Phys. Rev. B 18 (1978) 7165.
[45] M.W. Renner, K.M. Barkigia, D. Melamed, K.M. Smith, J. Fajer, Inorg. Chem. 35 (1996) 5120, and references therein.
[46] J. Ancheyta, G. Betancourt, G. Marroquin, G. Centeno, L.C. Castañeda, F. Alonso, J.A. Muñoz, M.T. Gomez, P. Rayo, Appl. Catal. A 233 (2002) 159.